DOI: 10.1002/cbic.200900717

Directed Evolution of an Antitumor Drug (Arginine Deiminase PpADI) for Increased Activity at Physiological pH

Leilei Zhu,[a, b] Kang Lan Tee,[b] Danilo Roccatano,[b] Burcu Sonmez,[b] Ye Ni,[c] Zhi-Hao Sun,*[c] and Ulrich Schwaneberg*[a, b]

Arginine deiminase (ADI; EC 3.5.3.6) has been studied as a potential antitumor drug for the treatment of arginine-auxotrophic tumors, such as hepatocellular carcinomas (HCCs) and melanomas. Studies with human lymphatic leukemia cell lines confirmed that ADI is an antiangiogenic agent for treating leukemia. The main limitation of ADI from *Pseudomonas plecoglossicida* (PpADI) lies in its pH-dependent activity profile, its pH optimum is at 6.5. A pH shift from 6.5 to 7.5 results in an approximately 80% drop in activity. (The pH of human plasma is 7.35 to 7.45.) In order to shift the PpADI pH optimum, a directed-evolution protocol based on an adapted citrulline-screening protocol in microtiter-plate format was developed and validated. A proof of concept for ADI engineering resulted in a pH optimum of pH 7.0 and increased resistance under physiological and slightly alkaline conditions. At pH 7.4, variant M2 (K5T/D44E/H404R) is four times faster than the wild-type PpADI and retains ~50% of its activity relative to its pH optimum, compared to ~10% in the case of the wild-type PpADI.

Introduction

Arginine deiminase (ADI) is a potential cancer therapy agent for the treatment of arginine-auxotrophic tumors (e.g., hepatocellular carcinomas (HCCs) and melanomas). HCC accounts annually for approximately one million new cases worldwide. In the US the incidence rate of HCC is 8.6 (per 100 000 persons; 1992–2002) with a mortality rate of 6.5 due to the low responses of hepatoma to chemotherapeutic treatments.[1] Current research efforts are focused on ADI's in vivo inhibitory effect towards HCCs, leukemia, melanomas, and human umbilical vein endothelial cells (HUVEC),[2–4] clinical trials for HCC (phase III) and melanoma (phase I/II),[3,5] and PEG formulation of ADI to improve its efficacy as a clinical drug, including serum half-life and antigenicity.[6,7] ADI inhibited the growth of cultured leukemia cells at concentrations of 5–10 ng mL^{-1}, which were about 20–100 times lower than those of the L-asparaginase standard, thereby resulting in fewer side effects.[4,8] ADI's inhibitory effect on human lymphatic leukemia is speculated to be caused by arginine deprivation.[4]

ADIs catalyze the first step of the ADI pathway by hydrolyzing arginine to citrulline and ammonium. Several ADI genes have been identified, purified, and characterized from bacteria, Archaea, and some eukaryotes, excluding mammalian cells, and summarized in a recent review.[1] From a kinetic point of view, none of these ADIs is ideally suited for in vivo applications in humans under physiological conditions.

Protein engineering by rational design and directed evolution offers opportunities to tailor ADI properties to physiological conditions. An *ADI* isolated from *Pseudomonas plecoglossicida* CGMCC2039 (accession number: ABS70718; PpADI) has been employed in an *E. coli* expression system for directed ADI evolution. Directed-evolution approaches employ mainly *E. coli* strains as expression host due to their fast growth and high transformation efficiencies. The latter is a prerequisite for generating complex mutant libraries. Directed protein evolution has over the last decades become a versatile and successful approach for tailoring protein properties to industrial demands (mainly in chemical synthesis) and for advancing our understanding of structure–function relationships in enzymes. A directed-evolution experiment comprises iterative cycles of diversity generation and functional selection for improved variants. Only a few reports on phytases,[9] xylanases,[10] amylases,[11–13] and an alcohol dehydrogenase[14] described a shift in pH optimum when using directed-evolution algorithms. None of these directed-evolution campaigns targeted a medical application, and arginine deiminase has, to the best of our knowledge, not been altered in its pH activity/resistance by directed evolution.

Comparison of PaADI (*Pseudomonas aeruginosa*, pH optimum 5.6; His405) and MaADI (*Mycoplasma arginini* ADI, pH optimum 6.5, Arg397) led to speculation that the substitution

[a] *L. Zhu, Prof. Dr. U. Schwaneberg*
Lehrstuhl für Biotechnologie, RWTH Aachen University
Worringerweg 1, 52056 Aachen (Germany)
Fax: (+49) 241-80-22387
E-mail: u.schwaneberg@biotec.rwth-aachen.de

[b] *L. Zhu, Dr. K. L. Tee, Prof. Dr. D. Roccatano, B. Sonmez, Prof. Dr. U. Schwaneberg*
School of Engineering and Science, Jacobs University Bremen
Campus Ring 1, 28759 Bremen (Germany)

[c] *Dr. Y. Ni, Prof. Z.-H. Sun*
Key Laboratory of Industrial Biotechnology
Ministry of Education, Jiangnan University
Lihu Avenue 1800, 214122 Wuxi, Jiangsu (China)
Fax: (+86) 510-8591-8252
E-mail: sunw@public1.wx.js.cn

 © 2010 Wiley-VCH Verlag GmbH & Co. KGaA, Weinheim

of His by Arg might contribute to MaADI's increased pH optimum.[15] A sequence alignment of four ADIs (MaADI, MyADI *(Mycoplasma arthritidis* ADI), PaADI, and PpADI) shows that for both *Pseudomonas* ADIs, the synonymous amino acid positions (404 and 405) contain a His, whereas both *Mycoplasma* ADIs contain an Arg at corresponding positions. Interestingly, both *Mycoplasma* ADIs have a pH optimum that is approximately one pH unit higher than the two *Pseudomonas* ADIs.

In this study, we report the first directed ADI evolution protocol in which the pH profile of PpADI was shifted to higher pH values; this represents a conceptional proof that ADI properties can be tailored for the demands of in vivo treatment of arginine-auxotrophic tumors. Emphasis is given to a detailed description of the conditions of directed evolution (mutagenic and screening).

Results

PpADI screening system for citrulline production in microtiter plates

Two key performance parameters for identifying improved variants in microtiter-plate-based screening systems are the true standard variation and the linear detection range of the employed assay. The DAM-TSC assay for citrulline detection (Scheme 1) was selected for directed evolution of PpADI. The microtiter-plate-screening format was optimized for simplified handling by lowering the color-development temperature (55 °C instead of 100 °C), increasing the diacetylmonoxime concentration (~22-fold), and avoiding the use of the sensitizer thiosemicarbazide.[28] Standard deviations of the modified citrulline detection assay were reduced by optimizing expression and screening conditions (various autoinduction media and assay conditions, such as amount of cell, conversion time, and color-development procedure). The preferred combination (150 μL LS5052 autoinduction medium, 20 μL cell culture, 20 min conversion time, and 15 min color-development time) resulted in a true standard deviation of 12.8% after subtracting the background (Figure 1 A). Screening systems with standard deviations of around 10% have successfully been used in directed-evolution experiments.[16,17] A wide linear detection window is important for identifying beneficial mutants in directed-evolution experiments, and screening systems for evolved mutants have to be constantly adapted so that they hit this window. A linear detection range up to 6 mM citrulline could be detected (Figure 1 B); a concentration of up to 6 mM was detected in microtiter plate screens.

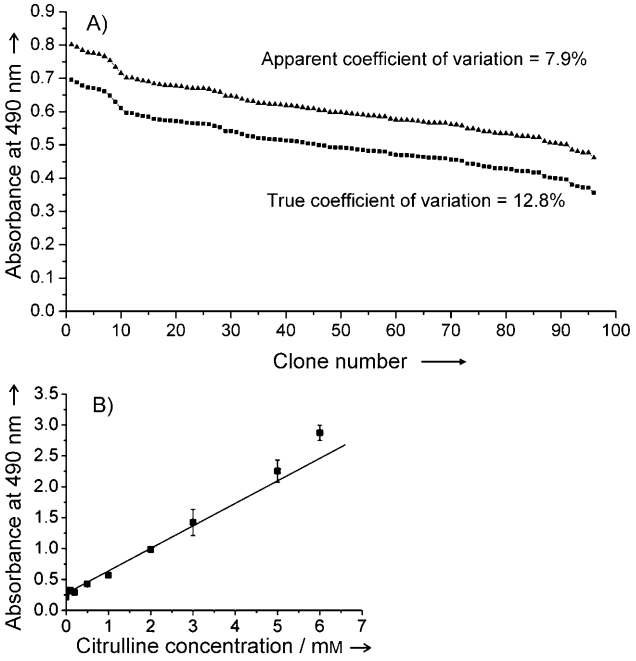

Figure 1. A) Activity values in descending order of the ADI wild-type conversion of arginine to citrulline in a 96-well microtiter plate by using optimized assay protocol. The apparent coefficients of variation were calculated without subtracting the background, and the true coefficients of variation were calculated after background subtraction. B) Calibration curve of 96-well microtiter-plate-format citrulline colorimetric screening assay.

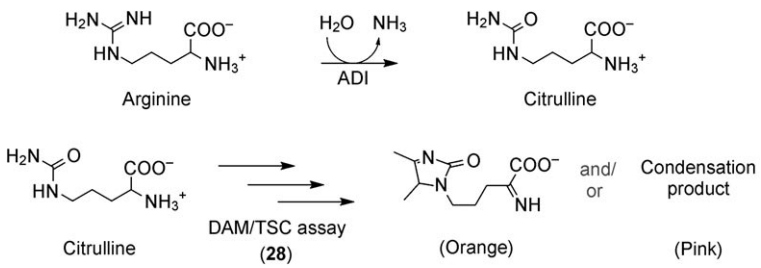

Scheme 1. Arginine conversion by ADI and detection of citrulline by using the DAM/TSC assay.

Validation of M1 (H404R) by using a cuvette-format citrulline colorimetric assay

Galkin et al.[15] proposed that a substitution of His at position 404 to Arg might influence ADI's pH profile. Compared to wild-type PpADI, variant M1 (H404R) shows higher activity (1.8-fold) and improved activity ratio at pH 7.4 to 6.4 (4.7-fold). Therefore, M1 was selected for directed evolution.

Validation of citrulline-production assay by screening error-prone mutant libraries

Various concentrations of $MnCl_2$ (0.01–0.10 mM) were used in epPCR library generation to adjust the ratio of active to inactive clones. A concentration of 0.01 mM $MnCl_2$, which generated 53% inactive mutants was selected for library generation. EpPCR mutant libraries with a ratio of 50% active and 50% inactive clones have often been used successfully in directed evolution, improving enzyme properties by gradual changes (one or two amino acids changes per round of mutagenesis and screening). A total of seven variants (Table 1) were identi-

 © 2010 Wiley-VCH Verlag GmbH & Co. KGaA, Weinheim

Table 1. Activity of ADI variants towards arginine determined by citrulline colorimetric assay in cuvette format. Samples were diluted to ensure that detected citrulline concentrations were within the linear detection range of the citrulline colorimetric assay. Wild-type, mutant M1 and the "best variant" M2 are in bold, and prominent expression mutants (9-B3-1; 21-D5-1) are italicized.

ADI variants	Normalized [ADI][a,b] Citrulline production [mM mg^{-1}]		Relative to activity of WT at pH 7.4		Activity ratio[b,c]
	pH 7.4	pH 6.4	pH 7.4	pH 6.4	
WT	9.83	124.92	1.00	12.69	0.08
	(0.74)	(1.98)	(0.15)	(0.01)	(0.01)
M1	17.80	45.95	1.81	4.67	0.39
(H404R)	(0.49)	(0.87)	(0.06)	(0.02)	(0.02)
M2	38.99	39.20	3.96	3.98	0.99
(K5T/D44E/H404R)	(0.79)	(0.31)	(0.02)	(0.02)	(0.03)
9-B3-1	24.89	54.50	2.53	5.54	0.46
	(0.45)	(1.80)	(0.03)	(0.03)	(0.02)
21-D5-1	25.68	50.95	2.61	5.18	0.50
	(2.68)	(2.36)	(0.07)	(0.02)	(0.01)
15-G10-2	13.11	47.02	1.33	4.78	0.28
	(0.53)	(0.47)	(0.09)	(0.02)	(0.01)
2-H4-2	12.50	21.58	1.27	2.19	0.58
	(0.07)	(0.09)	(0.06)	(0.04)	(0.01)
1-G11-1	24.91	29.12	2.53	2.96	0.85
	(0.20)	(0.33)	(0.03)	(0.03)	(0.02)
24-E10-1	14.62	32.82	1.49	3.34	0.45
	(0.62)	(0.52)	(0.08)	(0.03)	(0.02)

[a] Based on quantification employing Agilent 2100 Bioanalyzer (Agilent Protein 230 Kit). [b] Standard error of triplicate measurements are given in brackets below each absolute and normalized value. [c] Activity at pH 7.4/activity at pH 6.4.

fied from an epPCR library of 2400 mutants and used for further characterization. The most active variant was sequenced, and two additional amino acid substitutions (K5T and D44E) were identified.

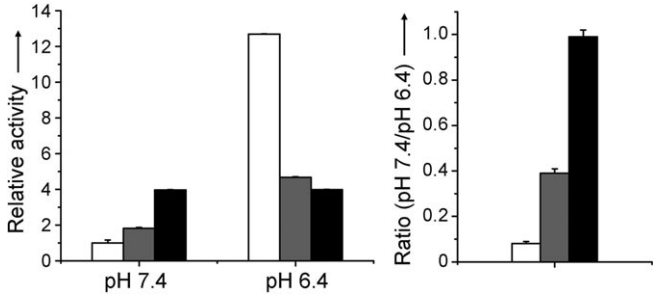

Figure 2. Relative activity of ADI variants towards arginine. Calculations are normalized against ADI quantifications recorded with the Agilent 2100 Bioanalyzer and Agilent Protein 230 Kit. The relative activity is the ratio of the activity at the pH of each variant relative to the activity at pH 7.4 of wild-type ADI. □: wild-type ADI, ■: M1 (H404R), ■: M2 (K5T/D44E/H404R).

Characterization of PpADI variants

Determination of k_{cat} *and* K_m *of wild-type ADI and the mutants*: Variants selected from epPCR were first characterized by using the crude cell extract to identify the most promising variants (Table 1). Using an activity ratio of pH 7.4 to 6.4 proved to be an effective method of eliminating expression mutants. Additionally, the concentration of PpADI and variants in the extract were determined by using the Agilent Protein 230 Kit to quantify differences in expression levels. Normalization of activities against the corresponding ADI concentrations revealed improvements in the specific activities of ADI mutants (Table 1). M1, the starting variant for the directed evolution campaign, and M2 were selected for detailed characterization studies. M2 has as "best identified variants" a more than 2.5-fold higher activity ratio at pH 7.4 to pH 6.4 than M1 and a twelvefold higher activity ratio than the wild-type in crude cell lysates (Figure 2).

For kinetic characterization of ADI variants, the citrulline production was maintained between 0.2–0.8 mM. The calibration curve in Figure 3 shows the linear detection range in the em-

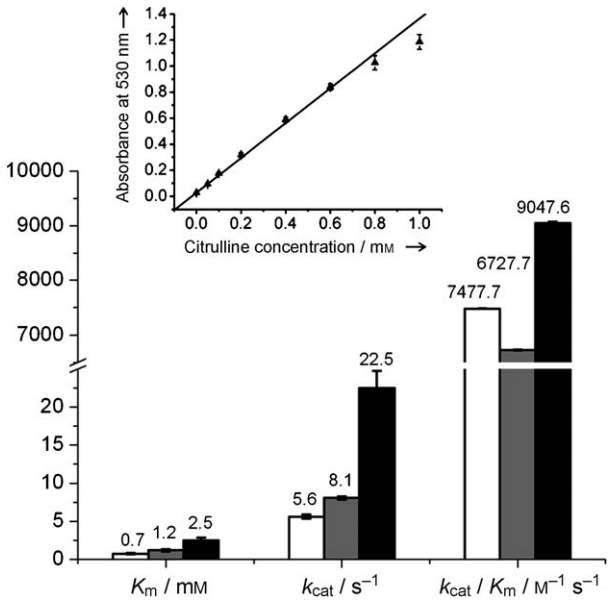

Figure 3. Kinetic parameters of ADI and mutants for conversion of arginine to citrulline. □: wild-type ADI, ■: M1 (H404R), ■: M2 (K5T/D44E/H404R). The values reported are the average of three measurements, and average deviations from the mean values are shown. The embedded calibration curve shows the linearity of the citrulline colorimetric assay in a 96-well PCR plate format, which was used to determine the arginine conversions and kinetic constants. The PCR-plate-format assay was performed in contrast to the directed-evolution screen at 70 °C, with thiosemicarbazide as sensitizer.

ployed 96-well PCR-plate-format citrulline colorimetric assay system. Figure 3 summarizes the k_{cat} and K_m values of wild-type PpADI, identified variants M1 (H404), and M2 (K5T/D44E/H404R), which were expressed in shaking-flask cultures and purified by using a two-step procedure (anion exchange followed by gel filtration). Both variants M1 and M2 show an increase in k_{cat} and K_m for citrulline production at pH 7.4. Variant M2 shows a fourfold higher k_{cat}, as also obtained by using the crude cell extract (Table 1); this validates the characterization procedure with crude cell lysate. Furthermore, an increase in K_m from 0.7 mM (wild-type PpADI) to 1.2 mM (M1) and 2.5 mM (M2) was found.

 © 2010 Wiley-VCH Verlag GmbH & Co. KGaA, Weinheim

Relative pH profile of wild-type and mutant

The pH profiles of wild-type PpADI and M1 (H404R) show identical pH optima at pH 6.5 (Figure 4); however, variant M2

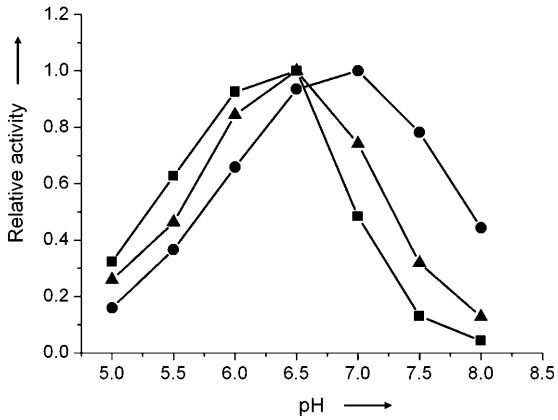

Figure 4. pH profile of wild-type PpADI (■), M1 (H404R) (▲), and M2 (K5T/D44E/H404R) (●). The relative activity is the ratio of the catalytic activity at that pH relative to the maximum activity of each enzyme. All pH profiles were recorded under arginine-saturated conditions (500 mM).

shows a pH optimum at pH 7.0, which is shifted remarkably (0.5 pH units). Both M1 and M2 show decreased specific activities at pH 6.5 and increased specific activity at pH 7.5. At pH 7.0, the specific activity of M2 exceeds that of wild-type PaADI by 20% (data not shown).

Discussion

ADI properties have to date not been engineered through directed evolution algorithms despite their often poor performance under physiological conditions and their potential antitumor importance. Chemically modified ADIs (e.g., through PEGylation)[1] and fusion proteins (e.g., human serum albumin fusion)[20] have been used to address activity and stability demands in vivo. Directed evolution offers opportunities to directly improve ADI properties for in vivo applications and small libraries of a few thousand variants have often been sufficient to find improved muteins in directed evolution experiments.[18,19]

Our main intention in this report is to provide a validated protocol for directed ADI evolution and improving the activity at the physiological pH 7.4. *Pseudomonas plecoglossicida* CGMCC2039 (PpADI, 7.8 U mg^{-1}; pH optimum 6.5) was selected for the directed evolution studies due to its functional expression in *E. coli*, coverage of sequence space in patents, and "potential" for activity improvement. PpADI is a relatively slow ADI when compared to *Mycoplasma* ADIs like MhADI (*Mycoplasma hominus* ADI, 35 U mg^{-1}), which would have been good alternatives for directed evolution studies.[1] Reported ADI activities range from 0.115 to 140.3 IU mg^{-1}. One unit is commonly defined as the amount of ADI that converts 1 μmol of L-arginine into 1 μmol of L-citrulline per minute.[1]

Screening of PpADI variants yielded three amino acid positions (5, 44, and 404). Only mutations at positions 44 and 404 resulted in a fourfold higher k_{cat} at pH 7.4 and a significant shift in the pH optimum (0.5 units) when compared to wild-type PpADI (Figures 3 and 4). Position 5 did not show any effect on PpADI activity.

Galkin and co-workers postulated that the histidine in position 404 (corresponding to position 405 in "their" PaADI) is a key residue in controlling activity at acidic and neutral pH. In the protonated state of the imidazolium ring, a hydrogen bond can be formed with the oxygen of Asp280 (carboxyl group). This hydrogen bond favors stabilizing interactions between Asp280 and the substrate arginine. His405 in PaADI was reported[15] to share protons with Asp280 and Glu13 and to be important for modulating the electrostatic environments of closely located catalytic groups. The same report postulated that H405 is likely to be protonated when the substrate arginine binds to the catalytic triad (His278, Glu224, Cys406).[22] Based on these reports, the His404 in PpADI was subjected to site-directed mutagenesis to Arg404 to give variant M1. M1 shows 40% residual activity compared to wild-type PpADI at pH 6.4, but a 1.8-fold increase in activity at pH 7.4 (see Table 1). In M1 (Figure 5A; based on PaADI 1RXX; residue His404 in PpADI corresponds to His405 in PaADI), the conformational effect due to the extended side chain of Arg likely weakens the hydrogen bond to Asp280 and thus reduces its stabilizing effect on arginine binding. As a result, the activity of M1 is reduced, especially at lower pH values at which His405 is protonated. However, at elevated pHs, His405 becomes increasingly deprotonated, whereas Arg405 remains protonated and can therefore still stabilize Asp280 for arginine binding. The electrostatic effect suggested by theoretical and experimental studies has shown the importance of positively charged resi-

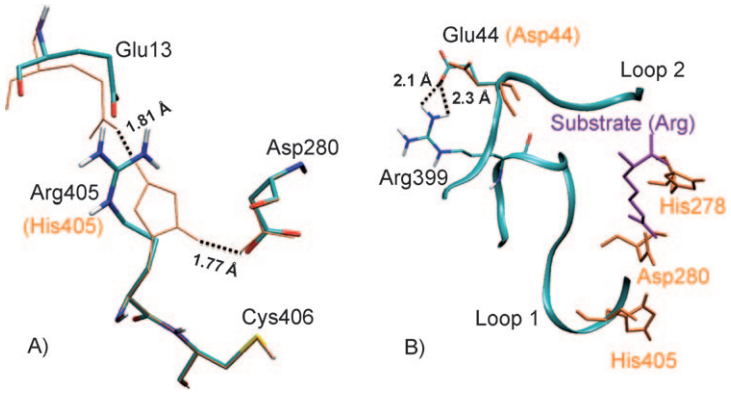

Figure 5. Structural alignment of two mutant models with corresponding residues of the crystal structures of the PaADI (in orange). A) The crystal structure of PaADI, which was diffracted in the absence of the substrate arginine (1RXX), was used to investigate the H405R substitution. Arg405 shows a different orientation with respect to the Asp280 of the guanidinium group from that of the side chain of His405 (in orange). B) The PaADI crystal structure in the presence of substrate arginine (2A9G) was used to investigate the role of the N44Q substitution. The latter was solved for an inactive variant in which Cys406 was replaced by Ala. The extended side chain of Glu44 might improve the hydrogen bond interaction with Arg399 by inducing a conformational shift of loop 1.

 © 2010 Wiley-VCH Verlag GmbH & Co. KGaA, Weinheim

dues to modulate the reaction rate of PaADI.[23] At pH 6.4, histidine in wild-type PpADI and arginine in M1 are both positively charged. At pH 7.4, histidine is only partially positive charged and PpADI's activity is reduced (>90%) while arginine in M1 remains positively charged, thus preserving M1's activity (Figure 4).

The PpADI H404R was used as starting variant for directed evolution. The epPCR library (2400 variants screened) resulted in a triple mutant M2 (K5T/D44E/H404R). In order to investigate the role of each position, the double mutants K5T/H404R and D44E/H404R were generated. Only D44E/H404R revealed improvements in k_{cat} (fourfold, pH 7.4). The rationale behind the effects of the D44E mutation on PpADI activity is more complex to extrapolate from the available ADI crystal structures. Comparative crystallographic studies have shown that the entrance to the active site is decorated with four loops that undergo conformational transitions upon arginine binding.[15] The loops exhibit significant shifts that limit the access of water molecules to the active site. Asp44 is located in loop 1 (residues 30–46) and, upon binding of the substrate, comes closer to the positively charged Arg399 located on loop 4 (residues 393–404). In the D44E mutant, the longer side chain reduce the distance to Arg399, thus favoring the formation of a hydrogen bond (Figure 5B). The reinforced interaction between Glu44 and Arg399 might expedite conformational changes in the loops, probably confining the arginine substrate in the active site, and hence promote arginine conversion. In the future, we plan to investigate further the influence of H404R and D44E using molecular-dynamics simulations, further boost the k_{cat} at pH 7.4, and reduce the K_m value of PpADI.

Overall site-directed mutagenesis of position H404R and one round of directed evolution (2400 variants screened) resulted in a triple mutant M2 (K5T/D44E/H404R) with fourfold higher k_{cat} at pH 7.4 (compared to wild-type; Figure 4). This, the best mutant isolated, has a specific activity of 31.3 U mg^{-1} at pH 7.4, which is already after one round of evolution close to the specific activity of MhADI (35 U mg^{-1})[21] at its pH optimum. The stability and specificity of improved PpADI variants are furthermore important for cancer treatment in vivo. First experiments in AB-human serum showed an unaltered stability of M2 compared to the wild-type PpADI. Furthermore, (N^G,N^G)-dimethylarginine conversion could not be detected with the citrulline colorimetric assay.

Conclusions

In summary, a directed-evolution protocol has been developed for PpADI and validated by increasing the k_{cat} of PpADI at physiological pH (7.4). The reported screening system is the first one employed in directed ADI evolution and can likely be used for other ADIs and other properties such as temperature stability, salt/detergent stability or protease resistance.

Experimental Section

Materials and methods: All chemicals were of analytical-reagent grade or higher quality and were purchased from Fluka, Sigma–Aldrich, and Applichem (Darmstadt, Germany), except the resins for purification (TOSOH, Stuttgart, Germany). All enzymes were purchased from New England Biolabs, Fermentas, and Sigma–Aldrich, unless otherwise stated.

Thermal cycler (Mastercycler gradient; Eppendorf) and thin-wall PCR tubes (Multi-ultra tubes; 0.2 μL; Carl Roth, Germany) were used in all PCRs. The PCR volume was always 50 μL except for Megaprimer PCR of whole plasmid (MEGAWHOP, 20 μL); larger volumes were prepared in multiple 50 μL PCRs. The amount of DNA in cloning experiments was quantified by using a NanoDrop photometer (NanoDrop Technologies, Germany).

Pseudomonas plecoglossicida CGMCC2039[24] was provided by Professor Zhihao Sun (Jiangnan University, Wuxi, China).

Reagents used in assays

Acid-ferric solution: Concentrated H_3PO_4 (70 mL, 85%) and concentrated H_2SO_4 (160 mL, 90–91%) were added slowly to dH_2O (600 mL). After the solution had been cooled to room temperature, $FeCl_3{\cdot}6H_2O$ (10 mL, 10 g L^{-1}) was added, finally the total volume was adjusted to 1 L with dH_2O.

Diacetyl monoxime-thiosemicarbazide (DAM–TSC) solution: Solutions of DAM (10 g L^{-1}) and TSC (0.3 g L^{-1}) in dH_2O were prepared separately, then mixed (1:1, *v/v*) just prior to use.

Cloning of ADI into pET42b(+): The *ADI* gene was amplified from *Pseudomonas plecoglossicida* CGMCC2039 by colony PCR (94 °C for 10 min, one cycle; 94 °C, 30 s/54 °C, 30 s/72 °C, 165 s, 29 cycles; 72 °C for 5 min, one cycle) by using primers 5′-CCG CAT ATG TCC GCT GAA AAA CAG AAG TAC GG-3′ and 5′-CTT CTC GAG TTA GTA GTT GAT CGG GTC GCG CAC G-3′, Pfu DNA polymerase (1.5 U), dNTP mix (0.20 mM), and a colony of *Pseudomonas plecoglossicida* CGMCC2039. The amplification product was purified by gel extraction, digested by using NdeI (20 U) and XhoI (20 U), and purified by using a QIAquick PCR purification kit (Qiagen). Cloning vector pET42b(+) was digested with NdeI (20 U) and XhoI (20 U), and purified by using a gel extraction kit (Qiagen). Digested *ADI* gene and pET42b(+) were ligated by using T4 DNA ligase (1 U) to give pET42b(+)–ADI and transformed into *E. coli* BL21-Gold (DE3). Sequence analysis of *ADI* showed that there was one synonymous mutation at Asp78 (GAT to GAC) compared to the ADI sequence of *Pseudomonas plecoglossicida* CGMCC2039 deposited in NCBI.

Site-directed mutagenesis of the *ADI* gene at position H404: Site-directed mutagenesis of the *ADI* gene was performed according to the published method[25] on plasmid pET42b(+)–ADI. The following oligonucleotides were used for the H404R mutagenesis: 5′-GGC CGT GGC GGC GGC CGT TGC ATG ACC TGC CCG-3′ and 5′-CGG GCA GGT CAT GCA ACG GCC GCC GCC ACG GCC-3′ (underlining indicated the substituted nucleotide). For the mutagenic PCR (First stage: 95 °C for 30 s, one cycle; 95 °C, 30 s/55 °C, 1 min/72 °C, 130 s, three cycles. Second stage: 95 °C for 30 s, one cycle; 95 °C, 30 s/55 °C, 1 min/72 °C, 130 s, 15 cycles; 68 °C for 30 min, one cycle), Phusion Hot Start DNA polymerase (2 U, Finnzymes, Keilaranta, Finland), dNTP mix (0.20 mM), each primer (25 pmol) together with template (p0ET42b(+) harboring *ADI*; 100 ng) were used. Following the PCR, DpnI (40 U; New England Biolabs) was added, and the mixture was incubated for 4 h at 37 °C. The PCR products were purified by using a QIAquick PCR Purification Kit (Qiagen) and transformed into *E. coli* BL21-Gold (DE3) for expression.

Construction of ADI error-prone library: The library was generated by the standard error-prone PCR (epPCR) with the improved variant H404R as template. For the mutagenic PCR (95 °C for 2 min,

 © 2010 Wiley-VCH Verlag GmbH & Co. KGaA, Weinheim

one cycle; 95 °C, 30 s/55 °C, 30 s/72 °C, 30 s, 29 cycles; 72 °C for 3 min, one cycle), Taq DNA polymerase (2.5 U), dNTP mix (0.20 mM), template (pET42b(+) harboring *ADI* H404R; 50 ng), $MnCl_2$ (0.01–0.1 mM), and 5′-TAC ATA TGT CCG CTG AAA AAC AGA AG-3′ and 5′-GTG CTC GAG TTA GTA GTT GAT CGG-3′ (10 pmol each) were used. The PCR products were purified by using a QIAquick PCR Purification Kit. The purified epPCR products were cloned into expression plasmid pET42b(+) by MEGAWHOP.[26] For MEGAWHOP (68 °C for 5 min, one cycle; 95 °C for 5 min, one cycle; 95 °C, 1 min/55 °C, 1 min/68 °C, 13 min 30 s, 24 cycles; 68 °C for 30 min, one cycle), Taq DNA polymerase (1 U), Pfu DNA polymerase (0.1 U), dNTP mix (0.20 mM) together with template (pET42b(+) harboring ADI gene H404R; 200 ng) were used. Following the PCR, DpnI (40 U; New England Biolabs) was added, and the mixture was incubated (4 h; 37 °C). The MEGAWHOP products were transformed into *E. coli* BL21-Gold (DE3) for expression and screening.

Cultivation and expression in 96-well plates: Colonies grown on LB_{kan} agar plates were transferred, by using toothpicks, into 96-well microtiter plates (flat-bottomed, polystyrene plates; Greiner Bio-One GmbH, Frickenhausen, Germany), containing LSG noninducing medium (150 μL)[27] supplemented with kanamycin (50 μg mL^{-1}). After 16 h of cultivation in a microtiter plate shaker (Multitron II, Infors GmbH, Einsbach, Germany; 37 °C, 900 rpm, 70% humidity), each well was replicated by using a replicator (EnzyScreen BV, Leiden, Netherlands) into a second series of 96-well microtiter plates containing autoinduction medium LS-5052 (150 μL)[27] supplemented with kanamycin (50 μg mL^{-1}). The first set of plates was stored at −80 °C after addition of glycerol. The clones in the second set of plates were cultivated for 12 h (Multitron II, Infors GmbH, 37 °C, 900 rpm) and used for screening.

Screening procedure

96-well plate-format citrulline colorimetric screening assay: A modified protocol for citrulline detection based on the carbamido-diacetyl reaction[28] (see Scheme 1 for assay mechanism) was used to measure the activity of ADI. Screening for increased activity was carried out by measuring the activities at pH 7.4 and 6.4.

Cell culture (20 μL) was transferred into 96-well microtiter plate. The enzyme reaction was initiated by the addition of arginine solution (100 μL, 100 mM) supplemented with cetyltrimethylammonium bromide (CTAB, 4 mM), and the mixture was incubated (20 min, 37 °C). Subsequently, acid-ferric solution (60 μL) and diacetyl monoxime (DAM, 20 μL, 0.5 M) were added. The reaction mixture was incubated for a further 15 min at 55 °C. Absorbance was measured at 492 nm on a microtiter plate reader (Tecan Sunrise, Tecan Group AG, Zürich, Switzerland).

Standard-deviation measurements were performed in 96-well plate format by using culture from BL21-Gold (DE3) lacking ADI and in a separate experiment containing ADI. Apparent standard deviation was based on the absolute absorbance values obtained from the ADI wild-type plate. The true standard deviation was calculated by subtracting the background absorbance value of the microtiter plate lacking ADI from the apparent values.

Cuvette-format citrulline colorimetric assay: ADI activity was routinely measured by using a modified citrulline-detection protocol with DAM and TSC[29] (see Figure 1 A for assay mechanism) in Eppendorf tubes. The enzyme reaction was initiated by the addition of arginine solution (200 μL, 100 mM) to a 2 mL Eppendorf tube containing crude cell lysate (50 μL), and the mixture was incubated for 20 min at 37 °C. Subsequently, acid-ferric solution (250 μL) was added to stop the enzyme reaction. After appropriate dilution with deionized water to ensure the concentration of produced citrulline was within linear detection range, the solution (400 μL) was mixed with acid-ferric solution (600 μL) and DAM-TSC solution (100 μL). The reaction mixture was incubated for a further 30 min at 70 °C, followed by incubation in ice water to stop color development. Absorbance was measured at 530 nm by using a Specord 200 (Analytik Jena AG, Jena, Germany).

Normalization of protein expression for wild-type ADI and variants: An Agilent Protein 230 Kit (Agilent Technologies Deutschland) and an Agilent 2100 Bioanalyzer were used to normalize protein expression in crude cell extract. The protocol used was according to the Agilent protein 230 Kit Guide, except BSA was used as an internal standard.

Expression of ADI in a shaking flask and purification: Shaking flasks (1 L) containing autoinduction medium LS-5052 (200 mL) supplemented with kanamycin (50 μg mL^{-1}) were inoculated with a 1:200 dilution of overnight culture (*E. coli* BL21-Gold(DE3) harboring pET42b-ADI) grown in noninducing medium LSG. After 12 h of expression, *E. coli* cells were harvested by centrifugation (Eppendorf 5810R 4 °C, 3220 *g*, 30 min) and resuspended in phosphate buffer (20 mL, Na_xPO_4, 20 mM, pH 7.0). *E. coli* cells were subsequently lysed by using a high-pressure homogenizer (1500 bar, two cycles; Avestin Emulsiflex, Mannheim, Germany). The disrupted cells were centrifuged (Eppendorf 5417R, 4 °C, 13000 *g*, 20 min), and the supernatant was further cleared by filtration through a low-protein-binding filter (0.45 μm; Minisart RC 25 single-use syringe filter; Sartorius, Hamburg, Germany). Wild-type ADI and mutants H404R and K5T/D44E/H404R were subsequently purified by column chromatography: 1) The filtered cell lysates were subjected to a Super-Q anion-exchange column that had been pre-equilibrated with phosphate buffer (Na_xPO_4, pH 7.0, 50 mM). Cell lysate (20 mL) was loaded. ADIs were eluted by a NaCl step elution in phosphate buffer (Na_xPO_4, pH 7.0, 50 mM) at a rate of 3 mL min^{-1}. 2) The ADI protein obtained by ion-exchange chromatography was subjected to a gel filtration column (Matrix: Toyoperl HW-55S, buffer: Na_xPO_4, pH 7.4, 50 mM, bed volume: 33 mL, bed height: 40 cm, column: Omnifit).

Purified ADI was subsequently concentrated in a Amicon ultra-4 centrifugal filter device (Millipore) with a 30 kDa cut-off membrane. The total protein concentration was determined by BCATM assay kit (Pierce, Born, Germany), and the homogeneity of the purified sample was controlled by SDS-PAGE by using standard molecular biology techniques.

Characterization of wild-type ADI and mutants

Determination of k_{cat} *and* K_m *of wild-type ADI and the mutants:* The k_{cat} and K_m values were determined from initial-velocity data measured as a function of substrate concentration. Enzyme reactions were carried out at 37 °C in a water bath. After 10 min of preincubation at 37 °C, the reaction was initiated by addition of purified enzyme (50 μL, 0.2–0.5 μM) to the substrate solution (200 μL, 0.2–10 mM of arginine, 0.5 M phosphate buffer, pH 7.4) in deep-well plates. The reaction mixture was incubated at 37 °C, and every 2 min an aliquot (30 μL) was transferred from each well to acid-ferric solution (30 μL) to stop the enzyme reaction. The color development was subsequently performed in a 96-well PCR plate. Ferric-acid solution (90 μL) and DAM-TSC solution (15 μL) were added to each well. The 96-well PCR plate was then incubated at 70 °C for 30 min in a thermal cycler (Eppendorf Mastercycler gradient) for color development, followed by incubation in ice water to stop color development. Absorbance was measured at 530 nm by using a microtiter plate reader (SPECTROstar Omega, BMG Labtech,

 © 2010 Wiley-VCH Verlag GmbH & Co. KGaA, Weinheim

Offenburg, Germany). The initial-velocity data obtained were fitted to the equation $v = v_{max}[S]/([S]+K_m)$ (where v is the initial velocity, v_{max} is the maximum velocity, [S] is the substrate concentration, and K_m is the Michaelis constant) by using GraphPad Prism software (GraphPad software, San Diego, CA, USA). The k_{cat} was calculated from the ratio of v_{max} and enzyme concentration.

Determination of pH profile: Enzyme reactions were carried out at 37 °C in a water bath using a solution of arginine (0.1 M) in phosphate (0.5 M)/acetate (50 mM) buffer (pH 5–8). After 10 min of preincubation at 37 °C, the enzyme reaction was initiated by adding purified enzyme (50 μL, 0.2–0.5 μM) to the substrate solution (200 μL) in deep-well plates. The reaction mixture was incubated at 37 °C for 10 min, and acid-ferric solution (250 μL) was transferred to each well to stop the enzyme reaction. The color development was subsequently performed in 96-well PCR plates. The reaction mixture (60 μL), ferric-acid solution (90 μL), and DAM-TSC solution (15 μL) were transferred to a 96-well PCR plate. The plate was then incubated at 70 °C for 30 min in a thermal cycler (Eppendorf Mastercycler gradient) for color development, followed by incubation in ice water to stop color development. Absorbance was measured at 530 nm by using a microtiter plate reader (SPECTROstar Omega).

Molecular modeling: Since a crystal structure of PpADI is not available, in order to gain first insights on the molecular level, two PaADI crystal structures (PDB ID: 1RXX, substrate-free; 2A9G, bound arginine) were used for structure analysis.[15] PpADI shares 84.9% sequence identity (http://blast.ncbi.nlm.nih.gov/Blast) with PaADI, and all reported ADIs show conserved substrate binding and catalytic residues. Residue His404 in PpADI corresponds to His405 in PaADI. Only one monomeric unit of the tetrameric PaADI was used for computational analysis employing Swiss–PDB viewer[30] (http://www.expasy.org/spdbv). PpADI M1 and PpADI M2, based on PaADI crystal structure, were generated by using the mutate command of Swiss–PDB viewer. Each side-chain rotamer with the best score was subsequently energy minimized by using the GROMOS96 force field in vacuo.[31]

Acknowledgements

The authors acknowledge financial support from Jacobs University Bremen and RWTH Aachen University to L.Z.

Keywords: antitumor agents · arginine deiminase · directed evolution · leukemia · pH optimum

[1] Y. Ni, U. Schwaneberg, Z. H. Sun, *Cancer Lett.* **2008**, *261*, 1–11.
[2] I. S. Park, S. W. Kang, Y. J. Shin, K. Y. Chae, M. O. Park, M. Y. Kim, D. N. Wheatley, B. H. Min, *Br. J. Cancer* **2003**, *89*, 907–914.
[3] F. Izzo, P. Marra, G. Beneduce, G. Castello, P. Vallone, V. De Rosa, F. Cremona, C. M. Ensor, F. W. Holtsberg, J. S. Bomalaski, M. A. Clark, C. Ng, S. A. Curley, *J. Clin. Oncol.* **2004**, *22*, 1815–1822.
[4] H. Gong, F. Zölzer, G. von Recklinghausen, W. Havers, L. Schweigerer, *Leukemia* **2000**, *14*, 826–829.
[5] L. J. Shen, W. C. Shen, *Curr. Opin. Mol. Ther.* **2006**, *8*, 240–248.
[6] C. M. Ensor, F. W. Holtsberg, J. S. Bomalaski, M. A. Clark, *Cancer Res.* **2002**, *62*, 5443–5450.
[7] F. W. Holtsberg, C. M. Ensor, M. R. Steiner, J. S. Bomalaski, M. A. Clark, *J. Controlled Release* **2002**, *80*, 259–271.
[8] H. J. Müller, J. Boos, *Crit. Rev. Oncol. Hematol.* **1998**, *28*, 97–113.
[9] A. Tomschy, R. Brugger, M. Lehmann, A. Svendsen, K. Vogel, D. Kostrewa, S. F. Lassen, D. Burger, A. Kronenberger, A. P. G. M. van Loon, L. Pasamontes, M. Wyss, *Appl. Environ. Microbiol.* **2002**, *68*, 1907–1913.
[10] O. Turunen, J. Janis, F. Fenel, M. Leisola, *Methods Enzymol.* **2004**, *388*, 156–167.
[11] T. Y. Fang, C. Ford, *Protein Eng.* **1998**, *11*, 383–388.
[12] C. Bessler, J. Schmitt, K. H. Maurer, R. D. Schmid, *Protein Sci.* **2003**, *12*, 2141–2149.
[13] A. Hirata, M. Adachi, S. Utsumi, B. Mikami, *Biochemistry* **2004**, *43*, 12523–12531.
[14] H. Sakoda, T. Imanaka, *J. Bacteriol.* **1992**, *174*, 1397–1402.
[15] A. Galkin, X. F. Lu, D. Dunaway-Mariano, O. Herzberg, *J. Biol. Chem.* **2005**, *280*, 34080–34087.
[16] T. S. Wong, F. H. Arnold, U. Schwaneberg, *Biotechnol. Bioeng.* **2004**, *85*, 351–358.
[17] A. Glieder, E. T. Farinas, F. H. Arnold, *Nat. Biotechnol.* **2002**, *20*, 1135–1139.
[18] K. L. Tee, O. Dmytrenko, K. Otto, A. Schmid, U. Schwaneberg, *J. Mol. Catal. B* **2008**, *50*, 121–127.
[19] Z. W. Zhu, C. Momeu, M. Zakhartsev, U. Schwaneberg, *Biosens. Bioelectron.* **2006**, *21*, 2046–2051.
[20] V. T. G. Chuang, U. Kragh-Hansen, M. Otagiri, *Pharm. Res.* **2002**, *19*, 569–577.
[21] H. Takaku, M. Matsumoto, S. Misawa, K. Miyazaki, *Jpn. J. Cancer Res.* **1995**, *86*, 840–846.
[22] X. F. Lu, L. Li, R. Wu, X. H. Feng, Z. M. Li, H. Y. Yang, C. H. Wang, H. Guo, A. Galkin, O. Herzberg, P. S. Mariano, B. M. Martin, D. Dunaway-Mariano, *Biochemistry* **2006**, *45*, 1162–1172.
[23] L. Li, Z. M. Li, C. H. Wang, D. G. Xu, P. S. Mariano, H. Guo, D. Dunaway-Mariano, *Biochemistry* **2008**, *47*, 4721–4732.
[24] Y. M. Liu, Z. H. Sun, Y. Ni, P. Zheng, Y. P. Liu, F. J. Meng, *World J. Microbiol. Biotechnol.* **2008**, *24*, 2213–2219.
[25] W. Y. Wang, B. A. Malcolm, *BioTechniques* **1999**, *26*, 680–682.
[26] K. Miyazaki, M. Takenouchi, *BioTechniques* **2002**, *33*, 1033–1038.
[27] F. W. Studier, *Protein Expression Purif.* **2005**, *41*, 207–234.
[28] R. M. Archibald, *J. Biol. Chem.* **1944**, *156*, 121–142.
[29] T. R. C. Boyde, M. Rahmatullah, *Anal. Biochem.* **1980**, *107*, 424–431.
[30] N. Guex, M. C. Peitsch, *Electrophoresis* **1997**, *18*, 2714–2723.
[31] W. F. van Gunsteren, S. R. Billeter, A. A. Eising, P. H. Hünenberger, P. Krüger, A. E. Mark, W. R. P. Scott, I. G. Tironi, *Biomolecular Simulation: the Gromos 96 Manual and User Guide*, ETH Zürich, **1996**.

Received: November 19, 2009
Published online on February 15, 2010

 © 2010 Wiley-VCH Verlag GmbH & Co. KGaA, Weinheim